Received: 7 October 2022 | Accepted: 2 November 2022

DOI: 10.1002/pamm.202200123

Application of the Coupled Eulerian Lagrangian method to the prediction of single-grain cutting forces in grinding

Tim Furlan[1,*], **Tountzer Tsagkir Dereli**[2], **Nils Schmidt**[2], **Dirk Biermann**[2], and **Andreas Menzel**[1,3]

[1] Institute of Mechanics, TU Dortmund University, 44227 Dortmund, Germany
[2] Institute of Machining Technology, TU Dortmund University, 44227 Dortmund, Germany
[3] Division of Solid Mechanics, Lund University, 22100 Lund, Sweden

Continuous technological advancements in the field of grinding technology and improved grinding tools have contributed to the development of high performance grinding processes. One example of such a process is internal traverse grinding (ITG) with electroplated cBN grinding wheels, where the tool consists of a conical roughing zone and a cylindrical finishing zone. Since the tool is fed in axial direction into a revolving workpiece, spindle deflections induced by varying process forces can lead to contour errors along the bore. Numerical simulations are a valuable tool to overcome the challenges associated with such high performance processes. Whenever spindle deflections need to be considered, accurate prediction of the process forces is paramount. Finite Element (FE) simulations have been widely used for the prediction of forces in cutting processes such as turning and milling, where only a small number of active cutting edges is considered, and where the geometry of these cutting edges is clearly defined. Grinding tools, on the other hand, contain a large number of grains with varying geometric characteristics. We recently proposed a multi-scale simulation system for the simulation of ITG processes, where a geometric kinematic grinding simulation, based on a database of digitalised grains of a real grinding wheel, was used to determine the grain engagements [1]. The process forces were obtained from summation of the contributions of all active grains at any given time, based on a force model on the individual grain level. The force model takes the material removal rate and an approximation of the rake angle into account, and was calibrated via finite element simulations.

In recent years, the Coupled Eulerian Lagrangian method (CEL), which is part of the commercial finite element software Abaqus, has been applied to simulate various cutting processes. No remeshing is necessary in this framework, and separation of chips from the workpiece can be modelled without element deletion. The application of CEL to the simulation of single grain cutting is therefore a promising approach to further improve the force model included in the process simulation of ITG. In this work, the kinematics of ITG are incorporated into a single grain cutting simulation, and the suitability of the CEL method for the problem is evaluated with a focus on the chip formation, separation and self-contact between the chip and the workpiece.

1 Introduction

Grinding processes play an important role in the industrial production of high-performance steel components. They are typically used as hard and fine machining processes after heat treatment of the workpiece and are often followed by fine-finishing processes, such as lapping or polishing [2]. At constant material removal rates high tool velocities are associated with reduced process forces, improved surface quality, and reduced tool wear. Due to the limitation by the bore diameter, internal grinding requires comparatively small tool dimensions, increasing the required rotational speed of the tool spindle for a given tool speed, and at the same time reducing the number of grains that participate in the cutting process. Therefore, usually only limited material removal rates can be achieved in internal grinding [3].

Internal traverse grinding (ITG) with electroplated cubic boron nitride (cBN) wheels is a high-performance process for the machining of bores. The tool is characterised by a split into a conical roughing zone and a cylindrical finishing zone and is fed in axial direction into the revolving workpiece. The material removal is realised mostly by the grains in the roughing zone, while the grains in the finishing zone improve the surface quality in the same stroke. Due to the unique process kinematics, the achievable material removal rates surpass those in hard turning while maintaining a better surface quality [4].

In general, the process normal force will induce a deflection between grinding wheel and workpiece according to the (usually very small) mechanical compliance of the system. Since the grinding wheel is not in contact with the full axial length of the workpiece at the same time, changes in the process forces occur during the process, which can result in shape deviations along the workpiece length. These shape deviations are especially relevant when no additional finishing takes place. Additional shape deviations might result from workpiece clamping and thermal effects [5].

An overview on the modelling of grinding processes is given in [6], where models are classified into seven categories: artificial neuronal networks, regression models, rule-based models, fundamental analytical models, kinematic models, finite elements based models, and molecular dynamics models. It is concluded that kinematic models provide the highest flexibility for different grinding operations or tools and, together with models based on finite elements or molecular dynamics, facilitate a higher level of understanding of the processes.

* Corresponding author: e-mail tim.furlan@tu-dortmund.de

In general, such kinematic models aim to approximate the interaction of each individual grain on the grinding wheel with the workpiece material but rely on simplified models for the interactions under consideration due to the large amount of grain engagements. We recently proposed a multi-scale simulation framework capable of simulating internal traverse grinding under consideration of elastic deflection between grinding wheel and workpiece, for which a model for the single-grain process forces was developed based on two-dimensional finite element cutting simulations [1]. The process forces could be predicted in good agreement with experimental observations, where the only experimental calibration was performed for the elastic compliance of the machining system.

A Lagrangian Finite Element scheme, based on the model presented in [5], was applied for the single-grain cutting simulations in [1]. Due to the large deformations during chip formation, a remeshing scheme is necessary for the simulations, which adds computational cost and introduces artificial diffusion of the solution variables.

Since the grain geometry is known in the single-grain simulations, models for cutting with geometrically defined cutting edge can be adopted. A comparison of the classic Lagrangian (LAG) and the Arbitrary Lagrangian Eulerian finite element method (ALE), smooth particle hydrodynamics (SPH), and the particle finite element method (PFEM) for the simulation of cutting identified SPH and PFEM as promising alternatives to the classic FE approaches since they maintain better distortion control and element quality under large deformations and include chip separation without techniques such as element deletion [7]. Another simulation approach that provides these advantages is the Coupled Eulerian Lagrangian finite element method (CEL), which is part of the commercial FE software Abaqus. CEL is a framework for fluid-structure interaction (FSI), providing a contact formulation between material moving through an Eulerian mesh and one or more Lagrangian bodies. When applied to cutting simulations, the workpiece material, which typically undergoes large deformations, is described in the Eulerian formulation, while the tool, often modelled as an elastic body, is described as a Lagrangian body. CEL has been applied to the simulation of orthogonal cutting in two dimensions, e.g. [8–10], and to the three-dimensional simulation of milling [11]. CEL-based three-dimensional simulations for single grain cutting experiments were proposed in [12]. However, the model is not directly applicable to internal grinding due to the linear kinematics, and no chip formation was shown.

The aim of this study is to evaluate the suitability of the Coupled Eulerian Lagrangian method for the simulation of single grain cutting in internal grinding processes. An approximation of the process kinematics is derived to include the influence of the varying depth of cut on the chip formation.

2 Single-grain force modelling

An ITG process for the grinding of a bearing component made of the bearing steel AISI 52100 with grains made of cubic boron nitride (cBN) is considered in order to investigate the suitability of the CEL method for the simulation of single grain cutting. Models of limited complexity are used for the plastic workpiece behaviour and the friction between workpiece and grains to focus on the applicability of the CEL method.

2.1 Process kinematics

Although the general simulation methods for single grain cutting in ITG are similar to those for orthogonal cutting, notable differences exist in the process kinematics. The relative path of the grain with respect to the workpiece surface is determined by the radius and the rotational speed of the grinding wheel (r_{t}, ω_{t}) and the workpiece (r_{wp}, ω_{wp}), the axial feed speed, as well as the maximum undeformed chip thickness $h_{\mathrm{cu,max}}$. Since the feed speed is typically small compared to the tool speed in ITG, we will only consider the velocities in the plane orthogonal to axial feed direction in the following. A schematic representation of the kinematics is presented in Fig. 1, and exemplary dimensions and velocities are given in Tab. 1.

The distance y_0 between the centre points of grinding wheel and workpiece is determined by the radii r_{t} and r_{wp}, and the maximum undeformed chip thickness $h_{\mathrm{cu,max}}$ as

$$y_0 = r_{\mathrm{wp}} - r_{\mathrm{t}} + h_{\mathrm{cu,max}} \, . \tag{1}$$

Assuming that the highest point of the grain lies exactly on the wheel radius, the position of this point with respect to the wheel centre can be expressed through the angle

$$\psi\,(t) = \psi_0 + \omega_t t \, , \tag{2}$$

where ψ_0 is the angle under which contact between grain and workpiece is established, and t is the time (where $t = 0$ for $\psi = \psi_0$ is assumed). Subtraction of the wheel radius from the current distance between wheel centre and grain tip then yields an approximation for the current depth of cut, i.e.

$$h_{\mathrm{cu}}\,(t) \approx \sqrt{r_{\mathrm{t}}^2 + y_0^2 + 2\, r_{\mathrm{t}} y_0 \sin\left(\psi\,(t)\right)} - r_{\mathrm{wp}} \, . \tag{3}$$

The angle of the grinding wheel normal (and therefore the grain) with respect to the workpiece surface normal follows as

$$\beta\,(t) = \psi\,(t) - \varphi\,(t) \tag{4}$$

with

$$\varphi(t) = \arctan\left(\frac{y_0 + r_t \sin(\psi(t))}{\cos(\psi(t))}\right). \tag{5}$$

Since $\beta(t)$ is small for realistic dimensions, the constant approximation for the relative tangential speed of the grain with respect to the workpiece surface

$$v_c \approx \omega_t r_t + \omega_{wp} r_{wp} \tag{6}$$

is admissible.

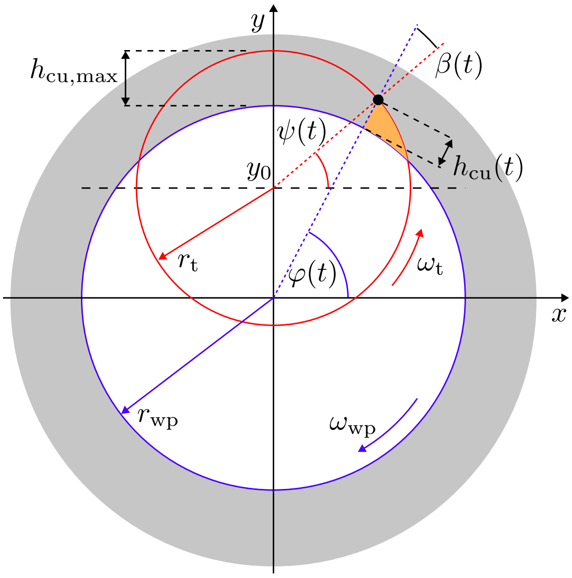

Fig. 1: Kinematics of the grain engagement in ITG (orthogonal to feed direction). The grinding wheel contour is depicted in red colour, while the inner contour of the workpiece before cutting is depicted in blue. The orange area marks the material that was removed by the grain at time t.

Table 1: Exemplary dimensions and velocities based on the grinding process for a bearing component.

Description	Symbol	Value	Unit
Grinding wheel radius	r_t	19.5	mm
Tool rotational speed	ω_t	4102.56	rad s^{-1}
Workpiece inner radius	r_{wp}	23.5	mm
Workpiece rotational speed	ω_{wp}	56.72	rad s^{-1}

2.2 Boundary value problem

In the CEL model, only a small section of the workpiece will be considered at any given time. Since the prescription of meaningful boundary conditions is considerably less complicated in a Cartesian coordinate system, and the angles under consideration are rather small, an approximation for the process kinematics in a Cartesian frame of reference is applied. Although the CEL method is implemented in three-dimensional elements, a plane strain problem can be set up by using a grid with a thickness of only one element, and restricting any flow normal to the considered plane through boundary conditions.

A tetrahedral mesh, obtained from measurements of a real cBN grain on a grinding wheel, is used for the grain. Since the focus of this study is on the applicability of the CEL method, it was not evaluated if the chosen grain geometry is representative for the grains on the wheel. Hexahedral CEL elements are used for the Eulerian domain, with a refined mesh towards the cutting zone. The workpiece is modelled by prescribing an initial workpiece material volume fraction of 1.0 in the corresponding part of the Eulerian mesh. An initial temperature of 293.0 K is prescribed for both the workpiece and the grain. Assuming a frame of reference that follows the grain in tangential, but not normal direction, the relative tangential speed between workpiece and grain is prescribed for the workpiece material through an initial condition and boundary conditions, while the current undeformed chip thickness $h_{cu}(t)$ and the relative grain angle $\beta(t)$ are prescribed through boundary conditions on the grain following Eqs. (3)-(4). A sketch of the boundary value problem is shown in Fig. 2.

Coulomb friction with a friction coefficient of 0.02 is assumed for the interaction between grain and workpiece. In general, the possibilities to model heat exchange between an Eulerian and a Lagrangian body with the CEL method are the same as with two Lagrangian bodies in Abaqus Explicit. However, since the workpiece surface is only implicitly defined through the volume fractions in the Eulerian elements, heat exchange with a surrounding medium can not be modelled in the same straight-forward way. Since the velocities are comparatively high in grinding, no heat exchange is considered in our model. However, workpiece material flowing out of the Eulerian domain will naturally transfer heat out of the system.

Since CEL is based on volume averaging, two streams of workpiece material will combine when contact is established between them. In the case of a chip touching the material flowing towards the cutting zone, the section of the chip touching

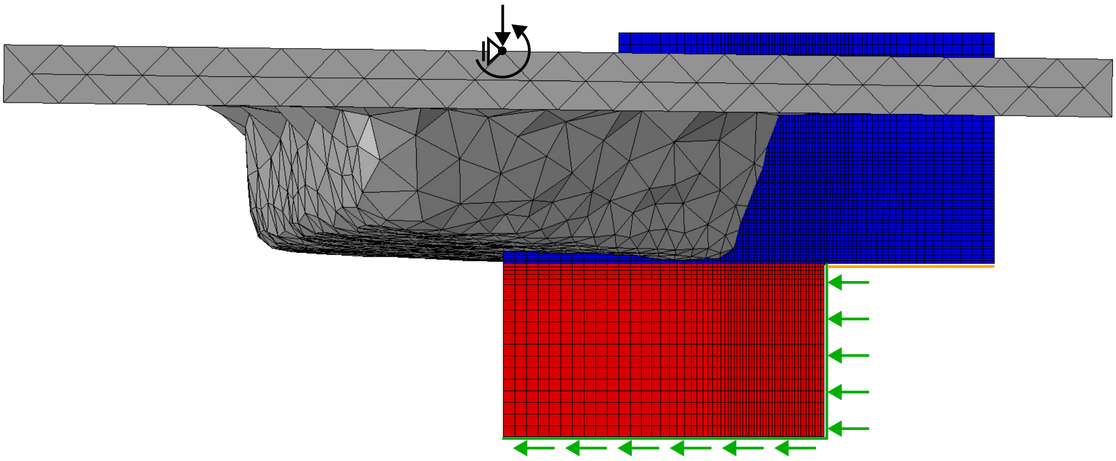

Fig. 2: Boundary value problem for the single grain cutting simulation in the initial configuration. Eulerian elements initially filled with workpiece material are coloured in red, while blue elements initially contain no material. Green arrows mark the prescribed speed at the Eulerian boundary, while the orange line marks the boundary where the chip will be reflected. The remaining boundaries of the Eulerian domain allow material outflow. The prescribed motion of the grain is indicated in black.

the workpiece will then be transported back towards the cutting zone, inducing an unphysical bending of the chip. The Eulerian domain is shaped in a way that prevents this self-contact. Instead of the workpiece, the chip contacts a boundary that prevents material outflow, acting as a rigid surface.

2.3 Material modelling

Since our study focuses on the applicability of the CEL method to single grain cutting, a comparatively simple material model was applied. The workpiece material is modelled as an isotropic continuum with thermo-elastic and thermo-viscoplastic contributions based on logarithmic strains and the well-established Johnson-Cook model [13]. The yield stress is given by

$$\sigma_{\mathrm{y}}^{\mathrm{JC}} = \left[A + B\left[1 - \mathrm{e}^{-\varepsilon_{\mathrm{p}} N}\right]\right]\left[1 + C\ln\left(1 + \frac{\dot{\varepsilon}_{\mathrm{p}}}{\dot{\varepsilon}_{\mathrm{p},0}}\right)\right]\left[1 - \left\langle\frac{\theta - \theta_0}{\theta_{\mathrm{m}} - \theta_0}\right\rangle^{M}\right] , \tag{7}$$

and is dependent on the accumulated plastic strain ε_{p}, the rate of the accumulated plastic strain $\dot{\varepsilon}_{\mathrm{p}}$, and the absolute temperature θ. Although local damage models can be included in the CEL framework, they are known to induce mesh dependencies of the results, and were therefore not included into the model to allow the examination of mesh convergence. Standard Fourier-type heat conduction is assumed in the workpiece material.

The Johnson-Cook model parameters A, B, C, M, N, and $\dot{\varepsilon}_{\mathrm{p},0}$, as well as the elastic and thermal parameters for the workpiece material, were chosen based on literature values for the steel alloy AISI 52100 proposed in [14]. Since no values were given for θ_{m} and θ_0 in [14], these were chosen following [15]. The cBN grain was modelled as rigid, since, at approx. $800\ \mathrm{GPa}$, the elastic stiffness of cBN is considerably higher than the stiffness of steel [16]. All material parameters are summarised in Tab. 2.

3 Results

The boundary value problem was solved for a maximum undeformed chip thickness of $h_{\mathrm{cu,max}} = 10\,\mu\mathrm{m}$ with different mesh densities. An exemplary temperature plot for the workpiece at two different times is shown in Fig. 3. The workpiece shape is approximated by an isosurface of the workpiece material fraction with value 0.5, while the grain is omitted for clarity of visualisation. Following the engagement of the grain with the workpiece, a distinct chip formation can be observed. The change in undeformed chip thickness throughout the process is reflected in the shape of the resulting chip, and leads to a separation of the chip from the workpiece towards the end of the engagement. Both the chip shape and the tangential force were compared between the different simulations, and element sizes graded between $1\,\mu\mathrm{m}$ and $4\,\mu\mathrm{m}$ were chosen as a good trade-off between accuracy and computational cost. Self-contact of the chip with the workpiece material flowing into the domain could be avoided after some trial and error by choosing an appropriate shape of the Eulerian domain.

Simulations were then performed with the maximum undeformed chip thickness ranging from $5\,\mu\mathrm{m}$ to $20\,\mu\mathrm{m}$. The calculated tangential force on the grain is shown in Fig. 4. Both the maximum of the tangential force and the duration of the grain engagement increase for larger values of $h_{\mathrm{cu,max}}$. In all simulations, a chip was formed, and separated from the workpiece towards the end of the simulation, leading to a vanishing tangential force.

Table 2: Summary of workpiece material parameters

Description	Symbol	Value	Unit
Mass density	ρ_{wp}	7.827×10^{-9}	$\mathrm{t\,mm^{-3}}$
Young's modulus	E_{wp}	7.827×10^{5}	MPa
Poisson's ratio	ν_{wp}	0.277	–
Johnson-Cook model parameters			
	A	688.17	Mpa
	B	150.82	Mpa
	C	0.3362	–
	M	0.0427	–
	N	2.7786	–
	θ_{m}	1780	K
	θ_0	298	K
	$\dot{\varepsilon}_0$	1	$\mathrm{s^{-1}}$
Thermal conductivity	λ_{wp}	46.6	$\mathrm{mW\,mm^{-1}K^{-1}}$
Specific heat*	$c_{\mathrm{p,wp}}$	$458 \ldots 798 \times 10^{6}$	$\mathrm{mJ\,t^{-1}K^{-1}}$
Thermal expansion coefficient*	α_{wp}	$11.5 \ldots 15.3 \times 10^{-6}$	$\mathrm{K^{-1}}$

*Temperature-dependent material parameters are linearly interpolated between the discrete literature values.

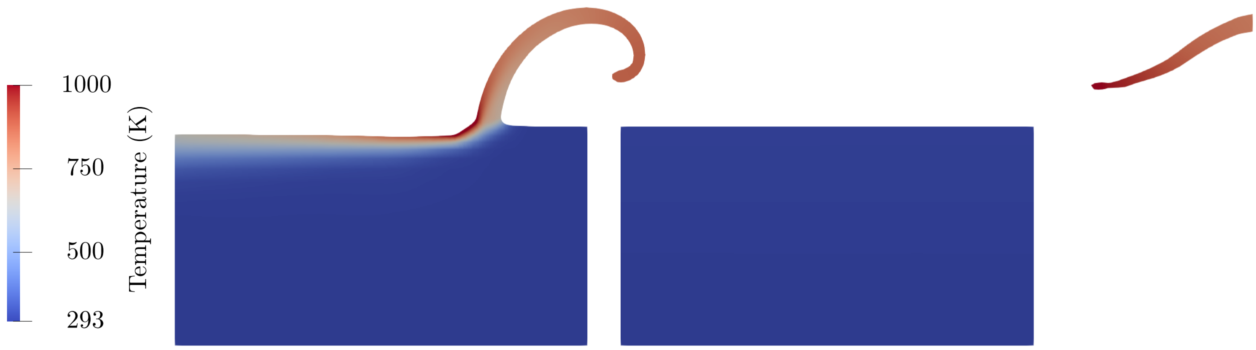

Fig. 3: Temperature distribution in the workpiece material at two times during the same simulation for a maximum undeformed chip thickness of $h_{\mathrm{cu,max}} = 10\,\mu\mathrm{m}$. The workpiece geometry is approximated by the isosurface of the workpiece material volume fraction with value 0.5. After the grain engages with the workpiece, a chip is formed, which increases in thickness as the undeformed chip thickness increases (left). When the grain moves out of the workpiece material, the chip thickness gradually reduces, and the chip finally separates from the workpiece (right). A significant temperature increase in the chip is visible, while the heat induced into the workpiece is transported out of frame by the motion of the material.

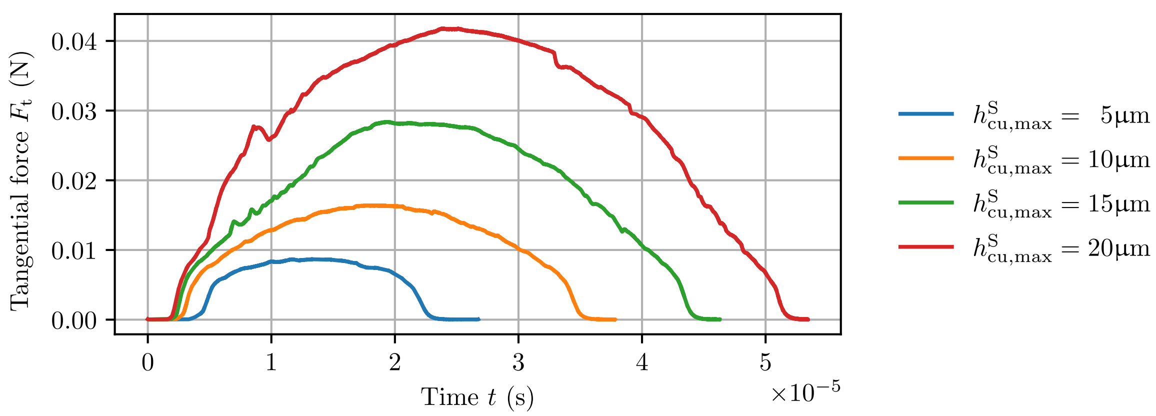

Fig. 4: Calculated tangential force F_{t} for different values of maximum undeformed chip thickness $h_{\mathrm{cu,max}}$. An exponential moving average filter was applied to reduce high-frequency oscillations.

4 Conclusion

The CEL method was combined with an approximation of the kinematics in single-grain cutting during ITG processes into a plane-strain model. Due to the characteristics of the CEL method, the framework can be used to simulate the formation of chips during the cutting process, as well as their separation from the workpiece, without remeshing or element removal techniques. However, the handling of workpiece material self-contact was identified as a drawback of the approach: When a chip comes into contact with the workpiece material flowing into the Eulerian domain, the surfaces of the chip and workpiece are merged, which results in a behaviour similar as if the chip was welded to the workpiece surface. Using an Eulerian domain mesh tailored to the chip morphology, self contact could be avoided in the simulation results presented in this study.

Some effect in the single-grain cutting process, such as ploughing, can not be predicted by using two-dimensional simulations. Although the presented model can be extended to the three-dimensional case in a straight-forward manner, and some preliminary work was already conducted in this regard, the treatment of self-contact in three dimensions poses a challenge. Apart from the extension to a fully three-dimensional setting, both damage and more advanced friction models shall be considered for more realistic simulation results. Another possible improvement to the model is the incorporation of heat transfer to the grain, as well as the inclusion of a second material phase to model heat transfer to a coolant medium. Based on these improvements, the framework can provide a suitable alternative to classic Lagrangian FE simulations for the prediction of single-grain forces in grinding processes.

Acknowledgements The funding provided by the German Research Foundation (DFG) under project number 403857741 is gratefully acknowledged. In addition, the authors thank their project partners at the companies Schaeffler Technologies AG & Co. KG and August Rüggeberg GmbH und Co. KG. The computer simulations were carried out on the Linux HPC cluster at TU Dortmund University (LiDO3), partially funded in the course of the Large-Scale Equipment Initiative by the German Research Foundation (DFG) as project 271512359. Open access funding enabled and organized by Projekt DEAL.

References

[1] T. Tsagkir Dereli, N. Schmidt, T. Furlan, R. Holtermann, D. Biermann, and A. Menzel, Simulation Based Prediction of Compliance Induced Shape Deviations in Internal Traverse Grinding, J. Manuf. Mater. Process. **5(2)**, 60 (2021). DOI: 10.3390/jmmp5020060.

[2] F. Hashimoto, H. Yamaguchi, P. Krajnik, K. Wegener, R. Chaudhari, Hans-Werner Hoffmeister and F. Kuster, Abrasive fine-finishing technology, CIRP Annals **65(2)**, pp. 597–620 (2016). DOI: 10.1016/j.cirp.2016.06.003.

[3] F. Klocke, Fertigungsverfahren 2. VDI-Buch. (Springer Vieweg, Berlin, Heidelberg, 2018), p. 222. DOI: 10.1007/978-3-662-53310-9

[4] K. Marschalkowski, D. Biermann and K. Weinert, On the Characteristics of High-Performance Internal Traverse Grinding Using Electroplated CBN Wheels, Mach. Sci. Technol. **16 (4)**, pp. 580–600 (2012). DOI: 10.1080/10910344.2012.731950.

[5] R. Holtermann, A. Menzel, S. Schumann, D. Biermann, T. Siebrecht, and P. Kersting, Modelling and simulation of Internal Traverse Grinding: bridging meso- and macro-scale simulations Prod. Eng. Res. Devel. **9**, pp. 451–463 (2015). DOI: 10.1007/s11740-015-0613-z.

[6] E. Brinksmeier, J.C. Aurich, E. Govekar, C. Heinzel, H.-W. Hoffmeister, F. Klocke, J. Peters, R. Rentsch, D.J. Stephenson, E. Uhlmann, K. Weinert and M. Wittmann, Advances in Modeling and Simulation of Grinding Processes, CIRP Annals **55 (2)**, pp. 667–696 (2006). DOI: 10.1016/j.cirp.2006.10.003.

[7] P. Sridhar, J.M. Rodríguez Prieto, and K.M. de Payrebrune, Discretization approaches to model orthogonal cutting with Lagrangian, Arbitrary Lagrangian Eulerian, Particle Finite Element method and Smooth Particle Hydrodynamics formulations, Procedia CIRP **93**, pp. 1496–1501 (2020). DOI: 10.1016/j.procir.2020.03.139.

[8] F. Ducobu, E. Rivière-Lorphèvre, and E. Filippi, Application of the Coupled Eulerian-Lagrangian (CEL) method to the modeling of orthogonal cutting, Eur. J. Mech. A. Solids **59**, pp. 58–66 (2016). DOI: 10.1016/j.euromechsol.2016.03.008.

[9] B. Peng, T. Bergs, F. Klocke, and B. Döbbeler, An advanced FE-modeling approach to improve the prediction in machining difficult-to-cut material, Int. J. Adv. Manuf. Technol. **103**, pp. 2183–2196 (2019). DOI: 10.1007/s00170-019-03456-0.

[10] T. Bergs, M. Hardt, and D. Schraknepper, Determination of Johnson-Cook material model parameters for AISI 1045 from orthogonal cutting tests using the Downhill-Simplex algorithm, Procedia Manuf. **48**, pp. 541–552 (2020). DOI: 10.1016/j.promfg.2020.05.081.

[11] A. Vovk, J. Sölter, and B. Karpuschewski, Finite element simulations of the material loads and residual stresses in milling utilizing the CEL method, Procedia CIRP **87**, pp. 539–544 (2020). DOI: 10.1016/j.procir.2020.03.005.

[12] F. Wöste, T. Siebrecht, M. Fast, and P. Wiederkehr, Geometric Physically-Based and Numerical Simulation of NC-Grinding Processes for the Calculation of Process Forces, Procedia CIRP **86**, pp. 133–138 (2019). DOI: 10.1016/j.procir.2020.01.022.

[13] G.R. Johnson and W.H. Cook, A Constitutive Model and Data for Metals Subjected to Large Strains, High Strain Rates, and High Temperatures, Proceedings of the 7th International Symposium on Ballistics, The Hague, The Netherlands, 1983, pp. 541–547.

[14] A. Ramesh and S.N. Melkote, Modeling of white layer formation under thermally dominant conditions in orthogonal machining of hardened AISI 52100 steel, Int. J. Mach. Tools Manuf. **48 (3-4)**, pp. 402–414 (2008). DOI: 10.1016/j.ijmachtools.2007.09.007.

[15] Y. Huang and S.Y. Liang, Force modelling in shallow cuts with large negative rake angle and large nose radius tools—application to hard turning, Int. J. Adv. Manuf. Technol. **22**, pp. 626–632 (2003). DOI: 10.1007/s00170-003-1550-0.

[16] J.S. Zhang, J.D. Bass, T. Taniguchi, A.F. Goncharov, Y. Chang, and S.D. Jacobsen, Elasticity of cubic boron nitride under ambient conditions, J. Appl. Phys. **109**, 063521 (2011). DOI: 10.1063/1.3561496.

